

# RSC Advances



This is an *Accepted Manuscript*, which has been through the Royal Society of Chemistry peer review process and has been accepted for publication.

*Accepted Manuscripts* are published online shortly after acceptance, before technical editing, formatting and proof reading. Using this free service, authors can make their results available to the community, in citable form, before we publish the edited article. This *Accepted Manuscript* will be replaced by the edited, formatted and paginated article as soon as this is available.

You can find more information about *Accepted Manuscripts* in the [Information for Authors](#).

Please note that technical editing may introduce minor changes to the text and/or graphics, which may alter content. The journal's standard [Terms & Conditions](#) and the [Ethical guidelines](#) still apply. In no event shall the Royal Society of Chemistry be held responsible for any errors or omissions in this *Accepted Manuscript* or any consequences arising from the use of any information it contains.

## ARTICLE

## Allylic oxidation of cyclohexene over ruthenium-doped titanium-pillared clay

Cite this: DOI: 10.1039/x0xx00000x

Ahmed Dali, Ilhem Rekkab-Hammoumraoui, Abderrahim Choukchou-Braham\* and Redouane Bachir

Received 00th December 2014,

Accepted 00th ..... 2014

DOI: 10.1039/x0xx00000x

www.rsc.org/

Ruthenium-doped H-Montmorillonite (H-Mont) and Ti-pillared clay (Ti-PILC) were prepared then studied for oxidation of cyclohexene, with tert-butylhydroperoxide (TBHP) as the oxygen source. The Ti-PILC support was prepared by hydrolysis of  $\text{Ti}(\text{OC}_3\text{H}_7)_4$  with HCl. The synthesized Ru/Ti-PILC and Ru/H-Mont catalysts were characterized by chemical analysis, surface area/pore volume measurements, Fourier transform infrared (FTIR) spectroscopy, X-ray powder diffraction (XRD), and UV-vis-diffuse reflectance spectroscopy (UV-vis-DRS). Both catalysts can selectively oxidize cyclohexene through allylic oxidation to give 2-cyclohexene-1-one as the major product, and 2-cyclohexene-1-ol as the minor product. The influence of reaction time, temperature, catalyst amount, and substrate/oxidant ratio was also investigated to find the optimal reaction for cyclohexene oxidation to get the highest conversion. Indeed, when the 5%Ru/Ti-PILC was employed as catalyst, 59 % of cyclohexene conversion, 87 % of selectivity for 2-cyclohexene-1-one and 13 % of selectivity for 2-cyclohexene-1-ol were obtained under ambient pressure, at 70 °C, for a 6 h reaction time. The catalysts were reused in four consecutive runs.

### 1. Introduction

Clay may be used as a catalyst in industrial processes of petroleum cracking, among others. However, only the external surface of the material is active in the catalysis, since large organic molecules cannot penetrate between its layers. In addition, the hydrophilic character of the layers does not allow access to apolar molecules, even those with reduced sizes<sup>1, 2</sup>. Pillared interlayered clays (PILCs) are two-dimensional zeolite-like materials, prepared by exchanging the charge-compensating cations between the clay layers with large inorganic cations, which are polymeric or oligomeric hydroxy metal cations, formed by hydrolysis of metal oxides or metal salts. Upon heating, the metal hydroxy cations undergo dehydration and dehydroxylation, thus forming stable metal oxide clusters which act as pillars that keep the silicate layers separated and create an interlayer space of molecular dimensions<sup>3</sup>. Compared with zeolites, PILCs possess the advantage of being new materials that can be tailored to particular applications by varying their composition as well as the size and separation of the pillars. A. Romero et al.<sup>4</sup> reported that a wide variety of factors can influence the intercalation/pillaring process. This situation leads to non-reproducible results, and makes it difficult to compare the results reported by different authors. These factors include the nature of the host clay used as the parent material, the nature of

<sup>a</sup> *Laboratoire de Catalyse et Synthèse en Chimie Organique, Faculté des Sciences, Université de Tlemcen, Algeria. mail : cba@mail.univ-tlemcen.dz*

the metallic cation, the hydrolysis conditions, the reaction time, the synthesis temperature and finally, the washing, drying and calcination processes. Research on titanium-pillared clays (Ti-PILCs) was initiated by J. Sterte<sup>5</sup> who first reported the synthesis of titanium - pillared montmorillonite, using  $\text{TiCl}_4$  in a hydrochloric acid solution. A. Bernier et al.<sup>6</sup> studied the influence of temperature on titanium-pillared clay by hydrolysis of  $\text{TiCl}_4$  in HCl. L. K. Boudali et al.<sup>7</sup> prepared titanium-pillared montmorillonite by intercalating montmorillonite with Ti by hydrolysis of  $\text{TiCl}_4$  in the presence of HCl or  $\text{H}_2\text{SO}_4$ . All the authors carried out detailed studies on the experimental conditions of the hydrolysis of  $\text{TiCl}_4$  with HCl. They indicated that the physicochemical properties of pillared clay depend on several synthesis parameters such as the concentration of metal ions and the method of preparation. S. Yamanaka et al.<sup>8</sup> reported the intercalation by hydrolysis of  $\text{Ti}(\text{OC}_3\text{H}_7)_4$ , in presence of HCl. The same procedure was used by B. M. Choudary et al.<sup>9</sup>. H. L. Del Castillo et al.<sup>10</sup> studied the effect of the nature of titanium alkoxides and the acid used in the hydrolysis phase. Recently, J. L. Valverde et al.<sup>11</sup> have reported the synthesis of titanium-pillared clay by varying the Ti precursors hydrolyzed by HCl. They studied the influence of the percentage of titanium added during the pillaring procedure, as well as the effect of the clay suspension concentration. These different methods have proven to be suitable for the preparation of titanium-pillared clays<sup>12</sup>. Titania modified clays have been found to be active catalysts, catalytic supports, photocatalysts and adsorbents for various environmental processes. They have been reported to be active

photocatalysts for NO<sub>x</sub> decomposition in polluted air<sup>13</sup>, and effective catalysts for the degradation of organic pollutants from waste water<sup>14, 15</sup>. It has also been reported that the elimination of H<sub>2</sub>S and SO<sub>2</sub> from waste gases was possible by using titania modified clays<sup>16, 17</sup>. Titania-pillared clay was found to be an effective sorbent for elemental mercury<sup>18</sup>. There are also a lot of reports describing the catalytic activity of clays modified with titania in the DeNO<sub>x</sub> process<sup>11, 19, 20</sup>.

The Allylic oxidation of olefins to  $\alpha,\beta$ -unsaturated ketones, particularly cyclohexene to 2-cyclohexene-1-ol and 2-cyclohexen-1-one, is an important and useful transformation in both chemical and pharmaceutical industries<sup>21-23</sup>, because they are derived directly from alkenes, a primary petrochemical source<sup>24</sup>. Many catalysts have been employed in cyclohexene oxidation, in recent years. For example, D. Habibi et al.<sup>25</sup> reported that the catalytic system SiO<sub>2</sub>/Al<sub>2</sub>O<sub>3</sub> nanosized-anchored ferrocene carboxaldehyde was investigated for the oxidation of cyclohexene by tert-butylhydroperoxide (TBHP). Fe-nano-catalyst showed higher cyclohexene conversion (> 84 %) with more than 90 % selectivity to 2-cyclohexene-1-one. K. Leus et al.<sup>26</sup> reported that Ti-functionalized NH<sub>2</sub>-MIL-47 was tested for the oxidation of cyclohexene, using molecular oxygen as oxidant in combination with cyclo-hexanecarboxaldehyde as co-oxidant. A cyclohexene conversion of approximately 25 % was observed for the bimetallic catalyst, after 6 h of reaction. S. J. J. Titinchi et al.<sup>27</sup> revealed that chromium complex supported on organically modified silica can catalyze the oxidation of cyclohexene by H<sub>2</sub>O<sub>2</sub>. The supported catalysts exhibited excellent activity (> 94%), after 6 h reaction time. When P. Bujak et al.<sup>28</sup> used Au/SiO<sub>2</sub> as catalyst, 67 % of cyclohexene conversion, 53.5 % of selectivity for 2-cyclohexene-1-one and 26.7 % of selectivity for 2-cyclohexene-1-ol were obtained. M. Vafaezadeh et al.<sup>29</sup> used the 1-Butyl-3-methylimidazolium tungstate ([BMIm]<sub>2</sub>WO<sub>4</sub>) ionic liquid supported onto silica; it displayed desirable performance for cyclohexene oxidation. A series of SiO<sub>2</sub>, Al<sub>2</sub>O<sub>3</sub> and TiO<sub>2</sub> mixed vanadium materials were tested by EL Korso et al.<sup>30</sup>, and the results showed that VO<sub>2</sub>-SiO<sub>2</sub> directs the reaction towards epoxidation. However, VO<sub>2</sub>-Al<sub>2</sub>O<sub>3</sub> leads it to an allylic oxidation. D. Lahcene et al.<sup>31</sup> reported a 46 % conversion when catalyst V<sub>2</sub>O<sub>5</sub>-TiO<sub>2</sub> was used. In the previously cited work, the porous TiO<sub>2</sub>-SiO<sub>2</sub> mixed metal oxide<sup>32</sup> was evaluated for the cyclohexene epoxidation with TBHP (tert-butyl hydroperoxide) as oxidant; the selectivity toward cyclohexene epoxide was 100 % and the conversion was 44 %. So far, the examples of catalytic allylic oxidation of cyclohexene in the presence of clays or pillared clays have been rare and to our knowledge, RuO<sub>2</sub> has not yet been used in any epoxidation reaction. However, only Ru complexes have been extensively used in numerous epoxidation reactions, such as the epoxidation of propene, octene, cyclohexene, cyclooctene, styrene, etc...<sup>33-37</sup>. Therefore, it would be interesting to extend the application of supported RuO<sub>2</sub>, for the first time, to the catalytic oxidation of cyclohexene.

Considering the fact that the porous structure and acidic character of PILCs make them attractive supports for catalyst preparation, we report, in the present paper, the preparation, characterization and catalytic oxidation behavior of ruthenium-clay catalysts. The samples were prepared by impregnation of titanium-pillared clay with several ruthenium precursors, and then characterized by physico-chemical techniques, such as the infrared spectral analysis, X-rays diffraction (XRD), specific surface area determination (BET) and UV-Vis DR Spectroscopy, in order to understand their behavior, and their performances as solid catalysts for the allylic oxidation of cyclohexene with

TBHP. The effect of reaction time, oxidant/cyclohexene ratio, amount of catalyst and temperature was examined as well.

## 2. Experimental

### 2.1. Catalysts synthesis

#### 2.1.1. Bentonite sample

The pillared clay was prepared using bentonite deposits from the Western town of Maghnia, in Algeria. Its chemical composition (mass %) was: SiO<sub>2</sub>, 69.4; Al<sub>2</sub>O<sub>3</sub>, 14.7; Fe<sub>2</sub>O<sub>3</sub>, 1.2; MgO, 1.1; K<sub>2</sub>O, 0.8; Na<sub>2</sub>O, 0.5; CaO, 0.3; TiO<sub>2</sub>, 0.2; and As, 0.05<sup>38</sup>. Mineralogical analysis showed that crude clay mineral contains mainly montmorillonite (85 %). The clay composition also includes quartz (10 %), cristoballite (4 %) and beidellite (1 %). The clay powder was purified according to the following procedure: clay dispersion was placed in a graduated cylinder to allow particles > 2  $\mu$ m in size to settle down, and the fine fraction, whose size was < 2  $\mu$ m, was extracted. Carbonates of calcium and magnesium were eliminated by hydrochloric acid (0.1 N) at the ratio of 10 mL g<sup>-1</sup>. The organic matter present in the clay sample was oxidized by addition of H<sub>2</sub>O<sub>2</sub> (33 %), at the ratio of 10 mL g<sup>-1</sup>, under agitation during 2 h, at ambient temperature. After centrifugation, purified clay was washed with distilled water until freed of Cl<sup>-</sup> ions, according to a test with AgNO<sub>3</sub>, then exchanged three times with H<sup>+</sup> ions by stirring in HCl solution (1 M) at 80 °C for 4 h. The resulting suspension was washed several times with distilled water until freed of Cl<sup>-</sup> ions, as indicated by the test with silver nitrate solution. The solid was separated by centrifugation and dried in air, at room temperature. This material is referred to as H-Mont.

#### 2.1.2. Ti-PILC

H-Mont was used in the pillaring process. Titania-pillared montmorillonite (Ti-PILC) was prepared as follows. The solution of titania oligocations was prepared by adding 90 mL of Ti(OC<sub>3</sub>H<sub>7</sub>)<sub>4</sub> (Aldrich, 98 %) to a solution of HCl (6.0 M, 18 mL). The mixture was diluted by slowly adding distilled water to reach the final concentrations of Ti<sup>4+</sup> and HCl equal to 0.82 M. The solution was aged at room temperature for 1 h. In the next step, the amount of pillaring agent required, to obtain the Ti/clay ratio of 10 mmol Ti per 1 g of clay, was added to the suspension which was then vigorously stirred. Montmorillonite was left in contact with the solution for 24 h and then separated by filtration. The obtained product was washed with distilled water, and then separated. This procedure was repeated until he modified montmorillonite was free of chloride anions, as determined by the test reaction with AgNO<sub>3</sub> solution. Finally, the modified clay was dried at 120 °C for 12 h and calcined at 400 °C for 4 h.

#### 2.1.3. Ruthenium supported Ti-pillared clays

These materials containing 5 wt.% of ruthenium, were prepared at room temperature under vigorous stirring, by incipient wetness impregnation of titanium-pillared clay support with a solution of Ru(acac)<sub>3</sub> dissolved in acetone. All the samples were then dried at 60 °C for 72 h, and calcined at 260 °C for 4 h, under air flow. The temperature was raised at the rate of 3 °C/min, and maintained at 260 °C, for 5 h.

## 2.2. Measurements

The Ru contents of catalyst samples were analyzed by atomic absorption spectrophotometer (AA300) (Perkin Elmer).

The cation exchange (CEC) capacity of purified clay was measured by exchange with cobaltihexamine chloride  $[\text{Co}(\text{NH}_3)_6]\text{Cl}_3$  as follows. An amount of 2 g dry weight of clay was placed in a tube and 40 mL of 0.05 N cobaltihexamine chloride solution was added. After continuous shaking for one hour, the content of the tube was centrifuged. Absorbencies at 472 nm ( $A_{472}$ ) were immediately measured. The  $A_{472}$  of the 0.05 N cobaltihexamine chloride solution was also determined. The whole experiment was repeated twice, and the 0.05 N cobaltihexamine chloride solution was freshly prepared before each CEC determination. According to L. Orsini and J. C. Rémy<sup>39</sup>, CEC can be derived from the concentration of Co remaining in the solution. As the cobaltihexamine chloride solution absorbs at 472 nm, the concentration of Co in the solution can be determined from  $A_{472}$  measurements. Considering the  $A_{472}$  of a solution of a given normality (i.e. 0.05 N), a  $\text{CEC}_{A_{472}}$  (meq 100 g<sup>-1</sup>) can be calculated as<sup>40</sup>:

$$\text{CEC}_{A_{472}} = \left[ \frac{A_{472_{0.05N}} - A_{472_{\text{sample}}}}{A_{472_{0.05N}}} \right] \times 50 \times \frac{V}{m} \times 100$$

where  $A_{472_{0.05N}}$  and  $A_{472_{\text{sample}}}$  correspond, respectively, to the absorbencies at 472 nm of 0.05 N (= 50 meq L<sup>-1</sup>) cobaltihexamine chloride solution and of clay sample; V: volume (L) of 0.05 N cobaltihexamine chloride solution added to the clay sample (0.04 L); m: mass of clay used (2 g).

The specific surface areas as well as the pore size distributions were determined by nitrogen adsorption at 77 K in a static volumetric apparatus (Quantachrome Instruments - Nova 1000<sup>®</sup>). Pillared clays were previously outgassed at 150 °C for 3 h. The total specific surface areas were calculated using the BET equation, whereas the total specific pore volumes were evaluated from nitrogen uptake at  $P = P_0 / 4$  0:99. The mesopore size distribution was obtained by applying the Barrett–Joyner–Halenda (BJH) method to the adsorption branch of the isotherm. The X-ray powder diffraction (XRD) patterns were measured on a Rigaku D/max2500 powder X-ray diffractometer. The diffractograms were recorded with a Cu  $K\alpha$  radiation ( $\lambda = 1.541874 \text{ \AA}$ ) in the range  $2\theta = 2^\circ - 70^\circ$ , with a step of  $0.02^\circ$  and an acquisition time of 1 s. The UV–visible spectra (200 – 800 nm) of these samples were collected on a Perkin Elmer UV/Vis spectrometer with an integrating sphere. The baseline was recorded using  $\text{BaSO}_4$  as a reference. The FTIR spectra of the samples were found using an Agilent Technologies Cary 600 series FTIR spectrophotometer, in the range 400 – 4000  $\text{cm}^{-1}$ . FTIR analysis of pyridine adsorption was carried out on an Agilent Technologies Cary 640 series FTIR spectrophotometer with a 4  $\text{cm}^{-1}$  resolution and a 4000–400  $\text{cm}^{-1}$  scanning range. The spectrometer was equipped with MCT detector cooled by liquid nitrogen. 18–20 mg of the catalyst sample was pressed into a self-supported wafer of approximately 2 cm in diameter, then evacuated at 623 K for 4 h, and finally cooled down to 293 K. A known amount of pyridine was then introduced in the cell at room temperature and the wafer was degassed at 423 K for 15 min to remove the physisorbed fraction. Finally pyridine adsorbed was followed by evacuation for 15 min at different temperature. The IR spectrum thus obtained was used to calculate

the amount of acid sites on the sample by measuring the peak area of pyridine adsorbed.

### 2.3. Catalytic evaluation of solids

The catalytic properties of Ruthenium supported Ti-pillared clays were determined in the liquid phase oxidation of cyclohexene, using tert-butyl hydroperoxide (TBHP) (Aldrich, 70 wt.% in  $\text{H}_2\text{O}$ ) as an oxidant. The reaction was carried out in a two-neck, round-bottom glass flask equipped with a magnetic stirrer and a reflux condenser. First, TBHP was stirred with heptane as solvent in order to perform a phase transfer from water to organic phase. Typically, 25 mL of heptane and 38.45 mmol (5.5 mL) of oxidant (TBHP) were mixed in a closed Erlenmeyer flask, magnetically stirred for 24 h. The organic phase was then separated from the aqueous phase. To control the phase transfer, the concentration of the remaining TBHP in the aqueous phase was determined by iodometric titration. Less than 10 % of the initial TBHP remained in the aqueous phase. In a typical heterogeneous catalytic reaction, the catalyst remains in suspension in 25 mL of the solvent (heptane), and the substrate (cyclohexene 29 mmol (3 mL)) was then added and heated at 70 °C, under vigorous stirring. The TBHP-solvent mix was subsequently added to the reaction mixture (time zero), and the resulting products were identified by comparison with the authentic ones. The course of reactions was then followed by gas chromatography (GC), using a Varian CP-3800 gas chromatograph equipped with a CP-WAX 52 CB and a flame ionization detector (FID). Before GC analysis, the remaining TBHP was decomposed by adding an excess of triphenylphosphine (Aldrich). On the other hand, to control the remaining TBHP, an iodometric titration was performed at the end of the reaction (after 6 h) by analyzing the organic phase.

## 3. Results and discussion

### 3.1. Characterization of the samples

The cationic exchange capacities (CEC), determined using a procedure reported in the literature<sup>39</sup>, were 89 mEq/100 g for natural clay and 34 mEq/100g for acidified clay. The XRD patterns of all samples are reported in Fig.1.

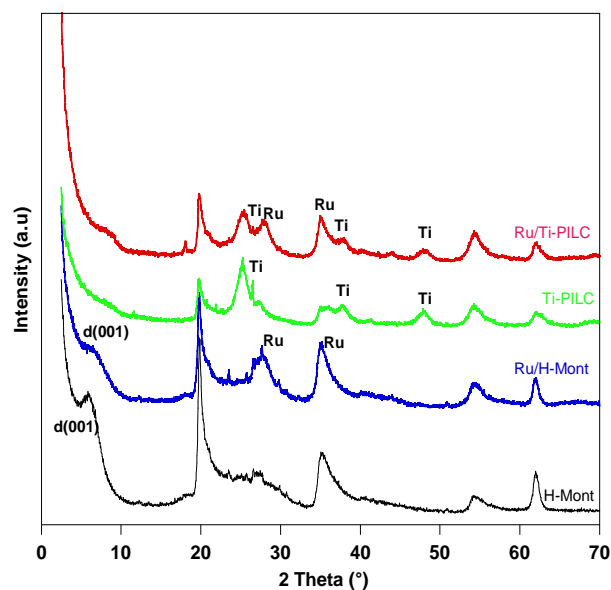


Fig. 1 X-ray diffractograms of samples

The XRD patterns of smectite clays generally show a basal (001) reflection and a two-dimensional diffraction (hk) only<sup>41</sup>. The (hk) reflections are characteristic of the type of clay mineral, whereas the 001 basal reflection is characteristic of the interlayer cations. The peaks, at angles 19.8 ° and 35 °, are assigned to the two-dimensional diffraction (hk) arising from the random stacking of clay layers. The diffraction at  $2\theta = 19.8^\circ$  is the summation of (hk) indices (02) and (11), while the diffraction at  $35^\circ$  is the summation of (hk) indices (13) and (20)<sup>16, 42</sup>. The basal spacing (001) reported for natural clay is about 1.5 nm<sup>43</sup>.

For H-Mont, the diffraction peak (001) attributed to the ordering of clay layers, was present at the position  $2\theta = 6.12^\circ$  which corresponds to the basal spacing of 1.44 nm.

The pillared clay sample Ti-PILC did not show the (001) peak. The absence of (001) peak in the lower region is due to the lack of a sufficiently ordered and oriented silicate layer structure. This indicates a highly disordered structure, which is the result of two phenomena. One is the non-uniform interlayer distances in clays; these are the results of inhomogeneous intercalation by small-sized Ti hydrolyzed species. The other is the disordered three-dimensional coaggregation of clay particles and Ti polyoxycations, i.e. the delaminated structure<sup>42, 44, 45</sup>. Similar results were observed in other pillared-clays<sup>44, 46, 47</sup>. Furthermore, the peaks at 25 °, 37 °, 48 ° and 53 ° are characteristic of anatase titania (JCPDS: 21-1272)<sup>4, 48</sup>.

After impregnation, Ru/H-Mont showed the basal reflection (001) at  $2\theta = 6.40^\circ$ . It indicates a distance of 1.37 nm between the layers of the material. This difference can be related to the degree of hydration of the cation type present in the clay structure<sup>49</sup>. In addition, Ru/Ti-PILC showed a low intensity of the peak, which presents a shoulder at the position  $2\theta = 8.5^\circ$ , characteristic of the basal spacing of 1.04 nm. This peak may be due to the intercalation of Ru nanoparticles in the interlayers of bentonite<sup>50</sup>. The appearance of peaks (reflections) at  $2\theta = 28^\circ$  and  $35^\circ$  indicates the presence of ruthenium oxide in our materials (JCPDS: 40-1290).

The FTIR spectra of purified clay (H-Mont) and pillared clay (Ti-PILC) samples are illustrated in Fig 2. The FTIR spectrum of H-Mont shows bands at 3642 and 3448 cm<sup>-1</sup> in the –OH stretching region; these two bands are assigned to the –OH stretching vibration of the structural hydroxyl groups in clay and water molecules present in the interlayer, respectively<sup>51, 52</sup>. On pillaring, these two bands broaden, due to the introduction of additional –OH groups; this is interpreted as a pillaring effect<sup>51-53</sup>. The band at around 1600 cm<sup>-1</sup> is assigned to the bending vibrations of water and Ti-OH<sup>54</sup>. The pillaring process replaces a large amount of interlayer cations that generally exist as hydrated; it also decreases the intensity of –OH peaks. Pillared clays have a low amount of adsorbed/coordinated water, due to their non-swellaible nature. Thus, as a result of pillaring, the intensity of the band around 1600 cm<sup>-1</sup> decreases<sup>55</sup>. The band around 1040 cm<sup>-1</sup> corresponds to the asymmetric stretching vibrations of SiO<sub>2</sub> tetrahedra<sup>56</sup>. The band at 524 cm<sup>-1</sup> can be ascribed to Si–O bending vibrations. On the other hand, the absorption bands associated with the Ru–O groups were observed at 442, 430, 428 cm<sup>-1</sup><sup>57</sup> and around 668 cm<sup>-1</sup><sup>58</sup>. In addition, a

peak was detected at 880 cm<sup>-1</sup>. The position of this peak corresponds to that of Ru=O<sup>54, 59, 60</sup>. The bands at 1457, 1540 and 2903 cm<sup>-1</sup> were only observed for Ruthenium supported catalysts; they can be assigned to the presence of –C=C, –C=O and –C–H groups, respectively. However, these bands are not observed in purified clay or pillared clay, which suggests that the acetylacetonate salt was not completely removed from supported samples after calcination.

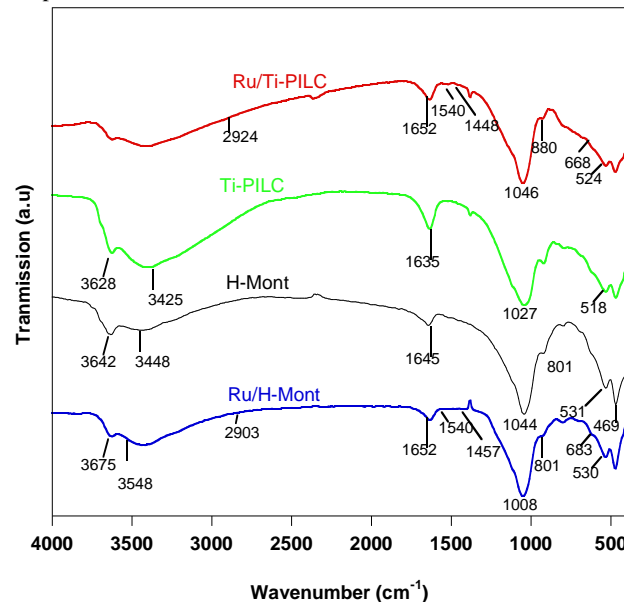


Fig. 2 FTIR spectra of samples

All samples showed a type IV isotherm according to IUPAC classification, which is typical of microporous materials, including mesopores<sup>61, 62</sup>. For all samples, the significant increase in adsorbed volume, at low relative pressures ( $P/P_0 < 0.01$ ), indicated the presence of micropores, while the H4 type hysteresis observed within the relative pressure range, from 0.40 to 0.99, showed the presence of mesopores. As an example, the isotherm of Ru/Ti-PILC is presented in Fig 3.

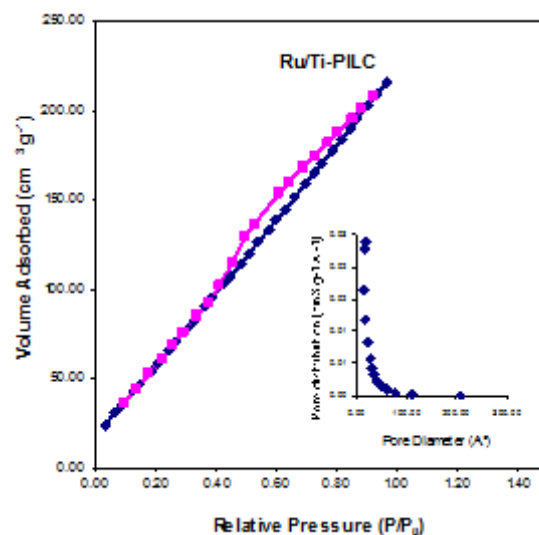


Fig. 3 N<sub>2</sub> adsorption–desorption isotherms and pore size distribution of Ru/Ti-PILC

The pore structure parameters, such as the specific surface area ( $S_{\text{BET}}$ ), the total porous volume ( $V_{\text{p}}$ ) and the pore diameter ( $d_{\text{p}}$ ) are summarized in Table 1. The BET surface area of Ti-PILC is  $278 \text{ m}^2 \text{ g}^{-1}$ , whereas that of the initial clay is  $195 \text{ m}^2 \text{ g}^{-1}$ . This suggests that the pillaring process leads to a dramatic increase in the porosity in layered clays. J. Arfaoui et al.<sup>12</sup> obtained the same BET surface area for Titanium-pillared clay.  $\text{TiO}_2$  particles are mainly located in the interlayer space as pillars, but it is also possible to find them on the external montmorillonite surfaces. After impregnation of the Ti-pillared clay with ruthenium, the BET surface area decreased sharply (Table 1). This effect can be explained by the blockage of some pores due to the building up of ruthenium on one side, and/or to the structural changes occurring during heat treatments on the other<sup>48</sup>. The pore volume also decreased after impregnation, indicating that ruthenium oxides blocked some small pores in H-Mont and Ti-PILC<sup>63</sup>.

As shown in the inset of Fig. 3, the BJH mesopore size distribution of all samples shows a unimodal and narrow peak, centered at  $19 \text{ \AA}$ .

**Table 1** BET surface area ( $S_{\text{BET}}$ ), total pore volume ( $V_{\text{p}}$ ) and pore diameter ( $d_{\text{p}}$ ) of samples

Catalysts	Ru loading (%)	$S_{\text{BET}}$ ( $\text{m}^2 \text{ g}^{-1}$ )	$V_{\text{p}}$ ( $\text{cm}^3 \text{ g}^{-1}$ )	$d_{\text{p}}$ ( $\text{\AA}$ )
H-Mont	/	195	0.27	19
Ti-PILC	/	278	0.33	19
5% Ru/ H-Mont	4.25	180	0.25	18
5% Ru/Ti- PILC	4.75	243	0.29	19

UV-vis-diffuse reflectance spectroscopy (UV-vis-DRS) is a technique suitable for studying the coordination environment of metal ions in constrained environments, such as in zeolites and clay materials. Fig. 4 illustrates the UV-vis-DRS spectra of the samples. H-Mont exhibits a characteristic broadband centered at about 250 nm, which is assigned to the ( $\text{Fe}^{3+} \leftarrow \text{O}^{2-}$ ,  $\text{OH}^-$ , or  $\text{OH}_2$ ) charge transfer band for the structural iron present in the octahedral layer of the clay mineral<sup>64-66</sup>. The absorption spectrum of Ti-PILC consists of three bands. The first one, which is located at about 315 nm, is characteristic of anatase clusters<sup>52</sup>; the band found at 215 nm is related to  $\text{Ti}^{4+}$  ions in a tetrahedral coordination<sup>67</sup>. In addition, the band at about 240 nm, which is due to the isolated extra-framework  $\text{Ti}^{4+}$  ions in octahedral coordination, was detected in this sample<sup>42</sup>.

The two clays (H-Mont and Ti-PILC) are almost transparent in the wavelength range beyond 400 nm; these same results were reported by S. Yang et al. and C. Ooka et al.<sup>65, 68</sup>.

UV-vis-DR spectra of H-Mont modified with ruthenium were deconvoluted into two new bands in the visible region: one at 526 nm and the second at 650 nm. These values correspond to the UV spectrum of  $\text{RuO}_2$ <sup>69, 70</sup>.

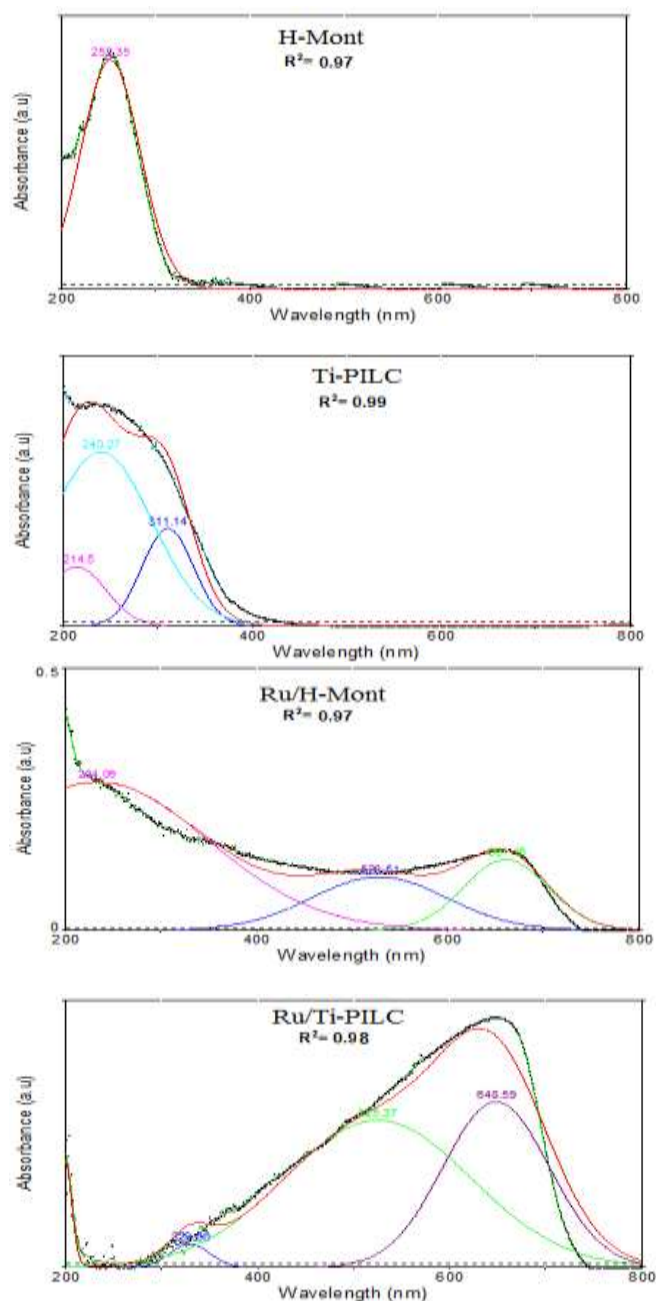


**Fig. 4** Diffuse-reflectance UV-Vis spectra deconvoluted bands

Fig. 5 presents representative IR spectra of all four samples, taken after their exposure to pyridine, which interacts differently with solid surface acid sites, depending on the nature of sites, i.e., Brønsted (Bpy) or Lewis (Lpy) sites. Species I (Lpy) is formed through coordinately bound pyridine, through its sole pair of electrons, on nitrogen atom to Lewis acid center, e.g.,  $\text{Al}^{+3}$  cations present on clay mineral surface. Species II (Bpy) is formed as a pyridinium ion, with a transfer of  $\text{H}^+$  ion from the Brønsted acidic  $-\text{OH}^{2+}$  groups of clay mineral to pyridine. Species III (Hpy) is formed as a result of hydrogen bonding between pyridine nitrogen atom and  $-\text{OH}$  groups of clay mineral. Pyridine vibration bands appear in the IR region, between  $1400$  and  $1700 \text{ cm}^{-1}$ . The Brønsted sites (Bpy) show bands near  $1490$ ,  $1540$ , and  $1635 \text{ cm}^{-1}$ . The  $1540 \text{ cm}^{-1}$  band is typical for this site; it corresponds to the pyridinium ion ( $\text{PyH}^+$ ). Pyridine coordinated to the Lewis sites (Lpy), absorbs near the bands at  $1455$ ,  $1490$ ,

and 1610–1625  $\text{cm}^{-1}$ ; the 1455  $\text{cm}^{-1}$  band is typical for these sites. The bands around 1440 and 1590  $\text{cm}^{-1}$  correspond to Hpy sites. A strong band at 1490  $\text{cm}^{-1}$  is attributed to pyridine associated with all acid sites, i.e., Lpy + Bpy + Hpy<sup>71</sup>.

A semi-quantitative measurement of Brønsted and Lewis acidities were carried out using the area of the characteristic Bpy band at 1545  $\text{cm}^{-1}$  and that of the characteristic Lpy band at 1455  $\text{cm}^{-1}$ <sup>72</sup>, to estimate the relative site density in the samples. In general, clay pillaring causes a considerable increase in acidity. The acid sites arise first from the exposure of the clay structure and second from the introduced pillar metal oxide. The addition of ruthenium oxide to Ti-PILC or to H-Mont increases the intensity of the peak at 1455  $\text{cm}^{-1}$ , which indicates an increase in the Lewis acidity. It was found that acid sites in all samples were predominantly Lewis acidic in nature. They can be ordered as follows: Ru/Ti-PILC > Ti-PILC > Ru/H-Mont > H-Mont.

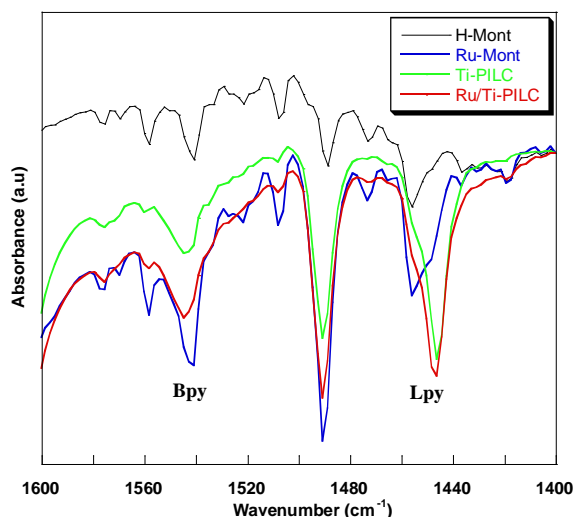
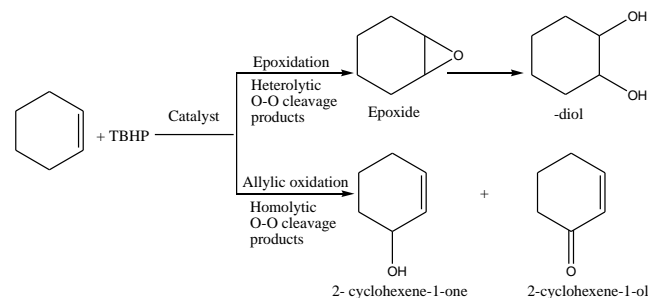


Fig. 5 Infrared spectra of pyridine adsorbed on samples

### 3.2. Catalytic activity study

To examine the catalytic activity of different catalysts, oxidation of cyclohexene was carried out using TBHP as oxidant. The possible reaction products are shown in Scheme 1. Oxidation of the double bond carbon-carbon of cyclohexene with peroxides yields the corresponding epoxide which upon further reaction with water, produces diols (Scheme 1). Oxidation of the allylic C-H bond results in alcohol (-ol) which can get further oxidized into a ketone product (-one)<sup>73</sup>.



Scheme 1 Oxidation products of cyclohexene

The main results are presented in Table 2, along with those of blank experiments. Both catalysts gave the unsaturated alcohol and ketone, 2-cyclohexene-1-ol and 2-cyclohexene-1-one. A blank oxidation reaction (i.e. without catalyst) was carried out under typical reaction conditions and no oxidation product was formed<sup>74,75</sup>. In order to show the effect of support on the catalytic activity, the reactions were repeated in the presence of Ti-PILC and H-Mont as catalysts, under the same reaction conditions.

Table 2 Cyclohexene oxidation in presence of catalysts and supports

Catalyst	Conv (%)	TBHP Consumption (%)	Selectivity (%)			
			2-cyclohexene-1-ol	2-cyclohexene-1-one	Epoxide	Diol
Blank	0	0	0	0	0	0
H-Mont	0	3	0	0	0	0
Ti-PILC	26	42	89	11	0	0
5% Ru/H-Mont	22	31	33	67	0	0
5% Ru/Ti-PILC	59	73	13	87	0	0

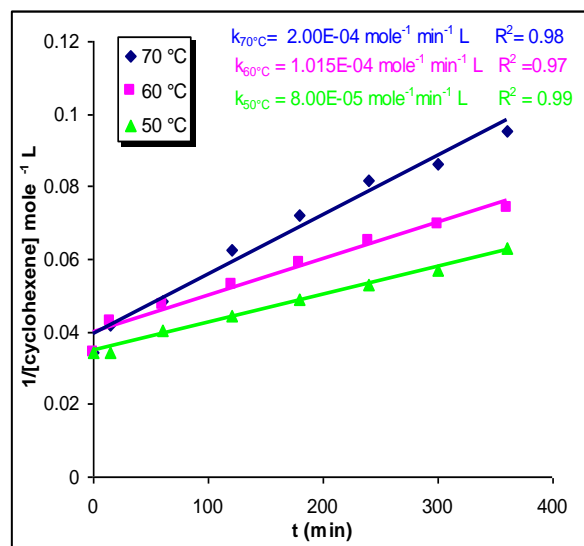
Reaction conditions: 29 mmol cyclohexene, 58 mmol TBHP, 20 mL heptane, 0.1 g catalyst, time: 6 h, reaction temperature 70 °C.

It was found that no conversion is observed in the presence of H-Mont as catalyst<sup>76</sup>, whereas Ti-PILC support exhibited a conversion of 26 %, with 89 % and 11 % selectivities for 2-cyclohexene-1-ol and 2-cyclohexene-1-one, respectively. It is clear that the incorporation of TiO<sub>2</sub> in the clay could further promote the catalyst activity and the products selectivity. M. I. Qadir et al.<sup>77</sup> found that TiO<sub>2</sub> promoted cyclohexene oxidation to yield cyclohexen-1-one and cyclohexen-1-ol. Layered clays have been extensively used as acid catalysts and as supports. IR spectroscopy showed that the metal oxide pillars are responsible

for the Lewis acidity; the Brønsted acid sites are located on the clay sheets<sup>78,79</sup>. On the other hand, TBHP as oxidant promotes the allylic oxidation pathway; however epoxidation is minimized, especially under the acidic properties of catalysts<sup>80-82</sup>.

By dispersion of ruthenium on H-Mont or Ti-PILC, cyclohexene was converted to 2-cyclohexene-1-one (67 % or 87 %) as the main product and to 2-cyclohexene-1-ol (33 % or 13 %). This means that the available ruthenium active sites were isolated; they increased the catalytic activity. Similar behaviors were observed by J. Arfaoui et al.<sup>83</sup> with vanadium supported Ti-

pillared montmorillonite catalyst in the oxidation of (E)-2-Hexen-1-ol. In this work, the only products of the reaction were 2-cyclohexene-1-one and 2-cyclohexene-1-ol. So, it can be concluded from the results that under the mentioned reaction conditions, the allylic hydrogen is more reactive than the C=C double bond. However, the abstraction of allylic hydrogen gives the corresponding radical; this requires a lower activation energy compared to that for the oxidation of the double bond. To obtain the best catalytic results, the effect of various parameters on the catalytic performance of 5% Ru / Ti-PILC, the most active catalyst, was investigated. On the other hand, the presence of a considerable number of these sites contributes both to the acidity of the solids and to the activity of the catalytic system. A similar finding was also reported by S. EL Korso et al.<sup>84</sup> in their study of VO<sub>2</sub>-SiO<sub>2</sub> catalyzed oxidation of cyclohexene. They concluded that increasing the strength of Lewis acid sites leads to allylic oxidation. M. Kim et al.<sup>85</sup> showed that by incorporating niobium pentoxide in Fe-pillared clay, both the thermal stability and surface acidity of the final catalyst Nb<sub>2</sub>O<sub>5</sub>/Fe-PILC were improved, hence resulting in a higher activity in H<sub>2</sub>S oxidation. From these results, it can be stated that our materials could be potential catalysts for certain applications that require the activation of the allylic position without affecting the double bond.



The influence of reaction temperature on the oxidation of cyclohexene over Ru/Ti-PILC catalyst was investigated in the temperature range between 50 and 70 °C. Beyond 70 °C, the decomposition or vaporization of TBHP proceeded suddenly<sup>86</sup>. The results are given in Table 3.

The reaction showed two major products, i.e. 2-cyclohexene-1-one and 2-cyclohexene-1-ol. The cyclohexene conversion increased to the maximum of 59 % at 70 °C. The reaction temperature also affected the distribution of the products. The selectivity to cyclohexenone went up with increasing temperature and reached the maximum of 87 % at 60 °C, and then remained almost unchanged at 70 °C while the selectivity to 2-cyclohexene-1-ol decreased. Similar observations were noted by M. Ghiaci et al. and X. Cai et al.<sup>87,88</sup> It can then be inferred that the reaction temperature of 70 °C is an optimum point to yield the highest ketone selectivities within the controllable reaction temperature interval. To test the order of the reaction, each of  $\ln [A]/[A]_0$  and  $1/[A]$  was plotted against  $t$ , for the reactions. The second order plots gave a straight line, indicating that the reaction is of 2<sup>nd</sup> order, as shown in Fig 5<sup>89</sup>. The activation energy, calculated from the slope of the straight line (Fig. 6), was found to be 42.09 kJ mol<sup>-1</sup>, which is lower than the values reported in several previous works (Table 4)<sup>90-93</sup>. However, P. Visuvamithiran et al.<sup>94</sup> and M. M. Taquikhan et al.<sup>95</sup> reported the same apparent activation energy.

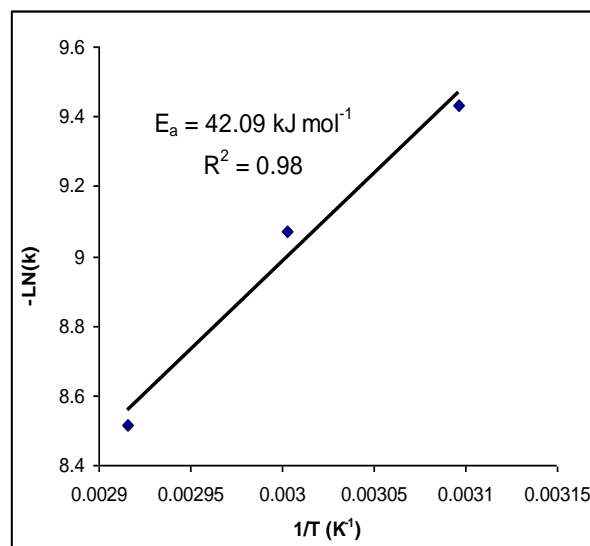
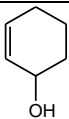
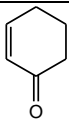
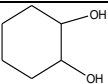


Fig. 6 Kinetic data at different temperatures and Arrhenius plot of the oxidation of cyclohexane

Table 3 Effect of reaction temperature on the conversion of cyclohexene and the selectivity of products.

Temperature (°C)	Conv (%)	TBHP Consumption (%)	Selectivity (%)			
						
50	38	51	50	50	0	0
60	48	57	14	86	0	0
70	59	73	13	87	0	0

Reaction conditions: 29 mmol cyclohexene, 58 mmol TBHP, 20 mL heptane, 0.1 g catalyst, 6 h.

**Table 4**  $E_a$  determined with different catalysts and different oxidants

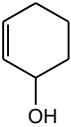
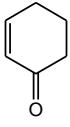
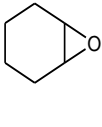
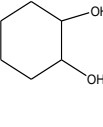
Catalyst	Oxidant	$E_a$ (kJ mol <sup>-1</sup> )	Source
MoO <sub>2</sub> (SAL-SH)DMF	O <sub>2</sub>	107.84	<sup>90</sup>
Uncatalysed		86.11	<sup>91</sup>
MnO <sub>2</sub>		54.34	<sup>92</sup>
Co-KIT-6	H <sub>2</sub> O <sub>2</sub>	40.13	<sup>94</sup>
Ru(III)-EDTA		35.95	<sup>95</sup>
PVMo/HMont		13.42	<sup>96</sup>
Mo- Cr- $\alpha$ Al <sub>2</sub> O <sub>3</sub>	TBHP	58.52	<sup>93</sup>
Ru/TiPILC		42.09	Present work

To study the effect of catalyst amount on the oxidation of cyclohexene, the quantity of catalyst Ru/Ti-PILC was varied from 50 to 200 mg, while keeping the other parameters fixed, i.e. cyclohexene (3 mL, 29 mmol), TBHP (58 mmol), heptane solvent (20 mL); the reaction was carried out at 70 °C, for 6 h. The results of the study, for three different amounts, are illustrated in Table 5. An

initial steep increase in cyclohexene conversion was observed when the amount of the catalyst was increased up to 100 mg. However, with further increase of the quantity of catalyst to 200 mg, the cyclohexene conversion decreased to 50 %, possibly due to adsorption or chemisorptions of the products on catalyst particles, thereby reducing the chance to interact. Similar observations were noted by S. Sharma et al. and S. K. Pardeshi et al.<sup>97,98</sup>. For different amounts of catalyst, 2-cyclohexene-1-one was found to be the major product. Its selectivity decreased from 89 % (50 mg) to 78 % (200 mg). Therefore, 100 mg was selected as the suitable amount of catalyst for oxidizing cyclohexene.

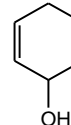
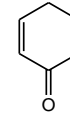
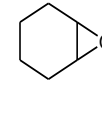
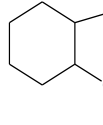
Investigation on the molar ratio of TBHP to cyclohexene (TBHP//Cyclohexene) was carried out, and the results are shown in Table 6. By increasing the TBHP to cyclohexene molar ratio, from 0.5 to 1.3, the reaction conversion increased from 15 % to 59 %, probably due to higher availability of oxidant molecules, while the product selectivity remained almost unchanged.

**Table 5** Effect of catalyst amount on cyclohexene conversion and products selectivity

Catalyst amount (mg)	Conversion (%)	TBHP Consumption (%)	Selectivity (%)			
						
50	17	21	11	89	0	0
100	59	73	13	87	0	0
200	50	66	22	78	0	0

Reaction conditions: 29 mmol cyclohexene, 58 mmol TBHP, 20 mL heptane, 6 h, reaction temperature 70 °C

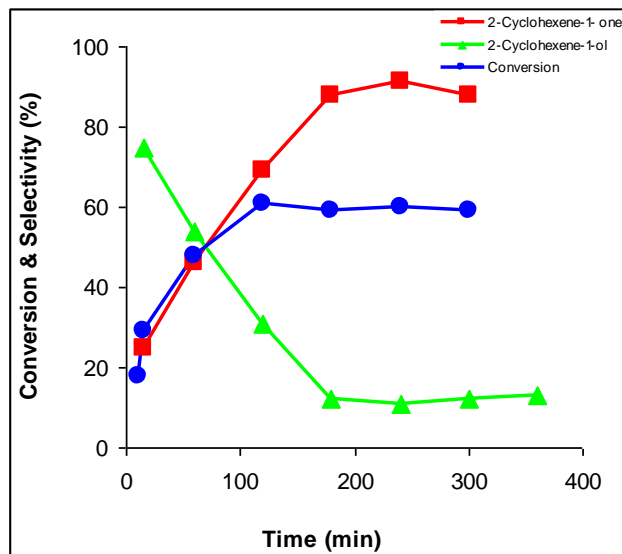
**Table 6** Effect of TBHP/Cyclohexene mole ratio on the conversion of cyclohexene and products selectivity

TBHP/Cyclohexene mole ratio	Conversion (%)	TBHP Consumption (%)	Selectivity (%)			
						
0.5	15	11	10	90	0	0
1.3	59	73	13	87	0	0
2	58	78	13	87	0	0

Reaction conditions: 29 mmol cyclohexene, 20 mL heptane, 0.1 g Ru/Ti-PILC catalyst, reaction time 6 h, reaction temperature 70 °C.

Ketone (2-cyclohexen-1-one) was always the main product (~87 %). Using RuO<sub>2</sub>/Co<sub>3</sub>O<sub>4</sub>/CeO<sub>2</sub> nanoparticles as catalyst, M. Ghiaci et al.<sup>87</sup> obtained the same results. A further increase in the molar ratio to 2 did not improve the reaction conversion or products selectivity. That means that each time a TBHP molecule is adsorbed, it reacts with the cyclohexene adsorbed on an adjacent site to form the ketone and alcohol, but the selectivity remains constant<sup>84</sup>. Therefore, the TBHP / Cyclohexene ratio of 1.3 is suitable to obtain satisfactorily high cyclohexene conversion and products selectivity.

The effect of reaction time on the oxidation reaction was investigated, and the results are shown in Fig. 7. As the reaction time increases, the cyclohexene conversion and selectivity of 2-cyclohexen-1-one increased rapidly, while the selectivity of 2-cyclohexen-1-ol decreased during the initial 180 min and then reached a plateau (from 3 h to 6 h). In pursuit of higher selectivity for the main product 2-cyclohexen-1-one, the reaction time of 3 h was considered as optimum.

**Fig. 7** Effect of reaction time on cyclohexene oxidation

Since the reusability of a catalyst is important from the economical and industrial points of view, we decided to investigate the reusability and stability of Ru/Ti-PILC in the oxidation reactions. The catalyst was easily isolated from the reaction mixture by simple filtration, after the catalytic reaction for the oxidation of cyclohexene. Then, a solvent was used to wash it, and recover it; it was finally dried at room temperature in order to be used for the next run, under the same reaction conditions.

As a typical example, the catalyst showed (Fig. 8) a conversion of 59 % in the first run, which decreased to about 52, 42 and 33 % in the 2<sup>nd</sup>, 3<sup>rd</sup> and 4<sup>th</sup> run, respectively. These results suggested that after the solvent washing the adsorbed compounds responsible of the decrease in the activity, were not fully removed over the catalyst surface and also to unavoidable loss of the catalyst during the process of collection.<sup>99</sup>

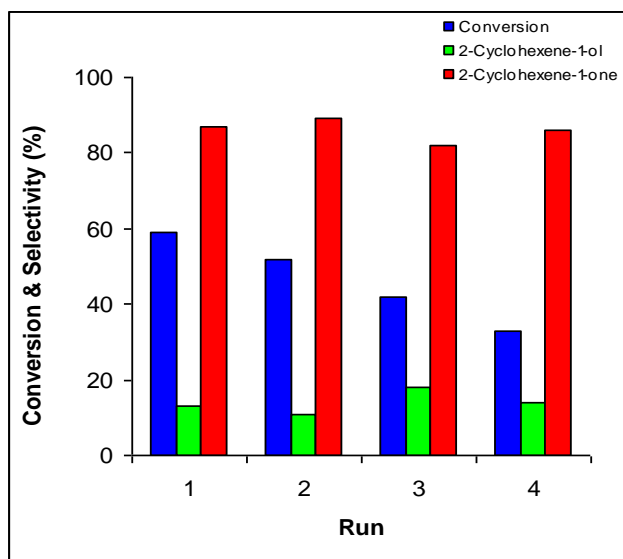


Fig. 8 Reusability of Ru/Ti-PILC in the oxidation of cyclohexene

The removed reaction mixtures were used to determine the ruthenium leaching. The results showed that the amount of ruthenium leached was 2 %, and the amount of leached metals from the catalyst was very low. Their contribution in the total catalyst activity, in the cyclohexene oxidation reaction, is probably negligible. The nature of the reused material was followed by DR UV-Vis spectrophotometry. The spectrum of the reused catalyst Ru/Ti-PILC showed no changes compared to the fresh one; this confirmed the stability of the catalyst.

## Conclusion

In this work, we presented the synthesis and characterization of ruthenium-doped titanium-pillared clay. The structure and surface properties of ruthenium on the support were examined using a variety of characterization techniques (UV-vis, FTIR, XRD). Pillaring of clay layers by titania resulted in an increase in the surface area, which enabled a better dispersion of the ruthenium species. This work allowed determining the catalytic activities of supports and catalysts on cyclohexene oxidation. To our knowledge, no reports about catalytic studies for Ru/supports have been mentioned yet. The results obtained show that cyclohexene was converted to 2-cyclohexene-1-one as the main product (59 % for Ru/Ti-PILC) and 2-cyclohexene-1-ol, within 3 h, with TBHP at 70

°C. The addition of ruthenium to the titanium-pillared clay increases the activities of PILC significantly.

Ru/Ti-PILC showed better effective catalytic activity than Ru/H-Mont. The influence of parameters like oxidant/substrate ratio, temperature, catalyst amount and reaction time were also investigated to find the optimal reaction on cyclohexene oxidation in order to get the highest conversion and selectivity. The reaction is second order and activation energy of 42.09 kJ mol<sup>-1</sup> is obtained. This activation energy is relatively better than several values reported in several previous works.

The reusability of the catalyst Ru/Ti-PILC showed that it retains its catalytic activity during the reaction and was reused more than four times without significant loss in its selectivity.

## Acknowledgements

The authors would like to thank the General Delegation for Scientific and Technical Research (DGRST) as well as the Thematic Research Agency for Science and Technology (ATRST), for the financial support to the project PNR-8-U13-880.

## References

1. S. Yamanaka, *Am. Ceram. Soc.*, 1991, **70**, 3.
2. S. M. D. Bosco, R. S. Jimenez, C. Vignado, J. Fontana, B. Geraldo, F. C. A. Figueiredo, D. Mandelli and W. A. Carvalho, *Adsorpt.*, 2006, **12**, 133-146.
3. A. Gil, L. M. Gandia and M. A. Vicente, *Catal. Rev.*, 2000, **42**, 145-212.
4. A. Romero, F. Dorado, I. Asencio, P. B. Garcia and J. L. Valverde, *Clay. Clay Miner.*, 2006, **54**, 737-747.
5. J. Sterte, *Clay. Clay Miner.*, 1986, **34**, 658-664.
6. A. Bernier, L. F. Admaia and P. Grange, *Appl. Catal.*, 1991, **77**, 269-281.
7. L. K. Boudali, A. Ghorbel, D. Tichit, B. Chiche, R. Dutartre and F. Figueras, *Microporous Mater.*, 1994, **2**, 537-541.
8. S. Yamanaka, T. Nishihara, M. Hattori and Y. Suzuki, *Mater. Chem. Phys.*, 1987, **17**, 87-101.
9. B. M. Choudary, V. L. K. Valli and A. D. Prasad, *J. Chem. Soc. Chem. Comm.*, 1990, 1186-1187.
10. H. L. Del Castillo, A. Gil and P. Grange, *J. Phys. Chem. Solids*, 1997, **58**, 1053-1062.
11. J. L. Valverde, A. de Lucas, P. Sanchez, F. Dorado and A. Romero, *Appl. Catal. B*, 2003, **43**, 43-56.
12. J. Arfaoui, L. Khalfallah Boudali and A. Ghorbel, *Catal. Commun.*, 2006, **7**, 86-90.
13. A. Nikolopoulou, D. Papoulis, S. Komarneni, P. Tsolis Katagas, D. Panagiotaras, G. H. Kacandes, P. Zhang, S. Yin and T. Sato, *Appl. Clay Sci.*, 2009, **46**, 363-368.
14. M. Fassier, C. S. Peyratout, D. S. Smith, C. Ducroquet and T. Voland, *J. Eur. Ceram. Soc.*, 2010, **30**, 2757-2762.
15. X. Yang, X. Ke, D. Yang, J. Liu, C. Guo, R. Frost, H. Su and H. Zhu, *Appl. Clay Sci.*, 2010, **49**, 44-50.
16. K. V. Bineesh, D. R. Cho, S. Y. Kim, B. R. Jermy and D. W. Park, *Catal. Commun.*, 2008, **9**, 2040-2043.
17. S. B. Rasmussen, R. Portela, S. Suarez, J. M. Coronado, M.-L. Rojas Cervantes, P. Avila and B. Sanchez, *Ind. Eng. Chem. Res.*, 2010, **49**, 6685-6690.
18. P. Worathanakul, P. Kongkachuichay, J. D. Noel, A. Suriyawong, D. E. Giammar and P. Biswas, *Environ. Eng. Sci.*, 2008, **25**, 1061-1070.
19. E. M. Serwicka, *Polish J. Chem.*, 2001, **75**, 307-328.
20. H. J. Chae, I. Nam, S. W. Ham and S. B. Hong, *Appl. Catal. B*, 2004, **53**, 117-126.

21. S. E. Dapurkar, H. Kawanami, K. Komura, T. Yokoyama and Y. Ikushima, *Appl. Catal. A*, 2008, **346**, 112-116.
22. D. Jiang, T. Mallat, D. M. Meier, A. Urakawa and A. Baiker, *J. Catal.*, 2010, **270**, 26-33.
23. R. M. Wang, Z. F. Duan, Y. F. He and Z. Q. Lei, *J. Mol. Catal. A*, 2006, **260**, 280-287.
24. D. B. Boyd, in *Ullmann's Encyclopedia of Industrial Chemistry*, ed. W. Wiley-VCH, 1998.
25. D. Habibi, A. R. Faraji, M. Arshadi and J. L. G. Fierro, *J. Mol. Catal. A*, 2013, **372**, 90-99.
26. K. Leus, G. Vanhaelewyn, T. Bogaerts, Y. Y. Liu, D. Esquivel, F. Callens, G. B. Marin, V. Van Speybroeck, H. Vrielandt and P. Van Der Voort, *Catal. Today*, 2013, **208**, 97-105.
27. S. J. J. Titinchi and H. S. Abbo, *Catal. Today*, 2013, **204**, 114-124.
28. P. Bujak, P. Bartzczak and J. Polanski, *J. Catal.*, 2012, **295**, 15-21.
29. M. Vafaezadeh, M. M. Hashemi and M. Shakourian Fard, *Catal. Commun.*, 2012, **26**, 54-57.
30. S. El-Korso, I. Rekkab, A. Choukchou-Braham, S. Bedrane, L. Pirault-Roy and C. Kappenstein, *Bull Mater Sci*, 2012, **35**, 1187-1194.
31. D. Lahcene, A. Choukchou-Braham, C. Kappenstein and L. Pirault-Roy, *Journal of Sol-Gel Science and Technology*, 2012, **64**, 637-642.
32. I. Rekkab-Hammoumraoui, K. Khaldi, A. Choukchou-Braham and R. Bachir, *Research Journal of Pharmaceutical, Biological and Chemical Sciences*, 2013, **4**, 935-946.
33. B. Scharbert, E. Zeisberger and E. Paulus, *J. Organomet. Chem.*, 1995, **493**, 143-147.
34. R. Antony, G. L. Tembe, M. Ravindranathan and R. N. Ram, *Polymer*, 1998, **39**, 4327-4333.
35. D. C. Sherrington, *Catal. Today*, 2000, **57**, 87-104.
36. V. R. de Souza, G. S. Nunes, R. C. Rocha and H. E. Toma, *Inorg. Chim. Acta*, 2003, **348**, 50-56.
37. D. Chatterjee, S. Basak, A. Mitra, A. Sengupta, J. Le Bras and J. Muzart, *Catal. Commun.*, 2005, **6**, 459-461.
38. B. Makhokhi, M. A. Didi and D. Villemin, *Mater. Lett.*, 2008, **62**, 2493-2496.
39. L. Orsini and J. C. Rémy, *Sci. Sol*, 1976, **4**, 269-275.
40. D. Aran, A. Maul and J. F. Masfaraud, *C. R. Geosci.*, 2008, **340**, 865-871.
41. S. W. Bailey, G. W. Brindley and G. Brown, *Structures of Clay Minerals and their X-ray Identification*, Mineralogical Society, London, 1980.
42. L. Chmielarz, Z. Piwowarska, P. Kustrowski, A. Wegrzyn, B. Gil, A. Kowalczyk, B. Dudek, R. Dziembaj and M. Michalik, *Appl. Clay Sci.*, 2011, **53**, 164-173.
43. L. S. Belaroui, J. M. M. Millet and A. Bengueddach, *Catal. Today*, 2004, **89**, 279-286.
44. J. P. Chen, M. C. Hausladen and R. T. Yang, *J. Catal.*, 1995, **151**, 135-146.
45. P. Yuan, X. Yin, H. He, D. Yang, L. Wang and J. Zhu, *Micropor. Mesopor. Mat.*, 2006, **93**, 240-247.
46. P. Yuan, X. Yin, H. He, D. Yang, L. Wang and J. Zhu, *Micropor. Mesopor. Mat.*, 2006, **93**, 240-247.
47. D. Chen, Q. Zhu, F. Zhou, X. Deng and F. Li, *J. Hazard. Mater.*, 2012, **235-236**, 186-193.
48. L. K. Boudali, A. Ghorbel, P. Grange and F. Figueras, *Appl. Catal. B*, 2005, **59**, 105-111.
49. F. C. A. Figueiredo, E. Jordao and W. A. Carvalho, *Appl. Catal. A*, 2008, **351**, 259-266.
50. W. Wang, H. Liu, T. Wu, P. Zhang, G. Ding, S. Liang, T. Jiang and B. Han, *J. Mol. Catal. A*, 2012, **355**, 174-179.
51. N. N. Binitha and S. Sugunan, *Micropor. Mesopor. Mat.*, 2006, **93**, 82-89.
52. K. V. Bineesh, D. K. Kim, H. J. Cho and D. W. Park, *J. Ind. Engin. Chem.*, 2010, **16**, 593-597.
53. K. V. Bineesh, D. K. Kim, D. W. Kim, H. J. Cho and D. W. Park, *Energy Environ. Sci.*, 2010, **3**, 302-310.
54. A. A. Ismail, D. W. Bahnemann and S. A. Al Sayari, *Appl. Catal. A*, 2012, **431-432**, 62-68.
55. L. Poppl, E. Toth, M. Toth, I. Paszli, V. Izvekov and M. Gabor, *J. Therm. Anal. Calorim.*, 1998, **53**, 585-596.
56. J. G. Carriazo, M. Moreno-Forero, R. A. Molina and S. Moreno, *Appl. Clay Sci.*, 2010, **50**, 401-408.
57. C. Potvin, J. M. Manoli, A. Dereigne and G. Pannetier, *J. Less-Common Met.*, 1971, **25**, 373-378.
58. J. S. Jeng, Y. T. Lin and J. S. Chen, *Thin Solid Films*, 2010, **518**, 5416-5420.
59. S. Hosokawa, Y. Fujinami and H. Kanai, *J. Mol. Catal. A*, 2005, **240**, 49-54.
60. E. H. P. Cordfunke and R. J. M. Konings, *J. Phase Equilib.*, 1993, **14**, 457-464.
61. S. Brunauer, L. S. Deming, W. E. Deming and E. Teller, *J. Am. Chem. Soc.*, 1940, **62**, 1723-1732.
62. F. Rouquerol, J. Rouquerol and K. Sing, in *Adsorption by powders and porous solids: principles, methodology and applications*, Academic Press, London, 1999.
63. F. C. A. Figueiredo, E. Jordao, R. Landers and W. A. Carvalho, *Appl. Catal. A*, 2009, **371**, 131-141.
64. J. Arfaoui, L. K. Boudali, A. Ghorbel and G. Delahay, *Catal. Today*, 2009, **142**, 234-238.
65. S. Yang, G. Liang, A. Gu and H. Mao, *Mater. Res. Bull.*, 2013, **48**, 3948-3954.
66. B. Gopal Mishra and G. Ranga Rao, *Micropor. Mesopor. Mat.*, 2004, **70**, 43-50.
67. A. Corma, *Chem. Rev.*, 1997, **97**, 2373-2420.
68. C. Ooka, H. Yoshida, K. Suzuki and T. Hattori, *Micropor. Mesopor. Mat.*, 2004, **67**, 143-150.
69. O. A. Blackburn, B. J. Coe, M. Helliwell, Y. T. Ta, L. M. Peter, H. Wang, J. A. Anta and E. Guillén, *Polyhedron*, 2013, **50**, 622-635.
70. M. Lenarda, R. Ganzerla, S. Enzo and L. Storaro, *J. Mol. Catal.*, 1991, **67**, 295-307.
71. L. Jankovic and P. Komadel, *J. Catal.*, 2003, **218**, 227-233.
72. S.P. Katdare, V. Ramaswamy and A.V. Ramaswamy, *Catal. Today*, 1999, **49**, 313-320.
73. T. Tatsumi, Y. Watanabe, Y. Hirasawa and J. Tsuchiya, *Res. Chem. Intermediat.*, 1998, **24**, 529-540.
74. A. Jana, S. Konar, K. Das, S. Ray, J. A. Golen, A. L. Rheingold, M. S. El Fallah, S. Mukherjee, S. Gupta, A. J. L. Pombeiro and S. K. Kar, *Polyhedron*, 2013, **62**, 51-60.
75. I. Y. Skobelev, A. B. Sorokin, K. A. Kovalenko, V. P. Fedin and O. A. Kholdeeva, *J. Catal.*, 2013, **298**, 61-69.
76. H. Salavati and N. Rasouli, *Mater. Res. Bull.*, 2011, **46**, 1853-1859.
77. M. I. Qadir, J. D. Scholten and J. Dupont, *J. Mol. Catal. A*, 2014, **383-384**, 225-230.
78. A. Corma and H. Garcia, *Chem. Rev.*, 2002, **102**, 3837-3892.
79. R. S. Varma, *Tetrahedron*, 2002, **58**, 1235-1255.
80. M. Salavati Niasari, M. Shaterian, M. R. Ganjali and P. Norouzi, *J. Mol. Catal. A*, 2007, **261**, 147-155.

81. G. von Willingh, H. S. Abbo and S. J. J. Titinchi, *Catal. Today*, 2014, **227**, 96-104.
82. M. R. Maurya, M. Kumar, A. Kumar and J. Costa Pessoa, *Dalton T.*, 2008, 4220-4232.
83. J. Arfaoui, L. K. Boudali and A. Ghorbel, *Appl. Clay Sci.*, 2010, **48**, 171-178.
84. S. El-Korso, I. Khaldi, S. Bedrane, A. Choukchou-Braham, F. Thibault-Starzyk and R. Bachir, *J. Mol. Cat. A*, 2014, **394**, 89-96.
85. M. Kim, G. Lee, D. Kim, D. Kang and D. Park, *Korean Journal Chemical Engineering*, 2014, **31**, 2162-2169.
86. K. M. Parida, M. Sahoo and S. Singha, *J. Mol. Cat. A*, 2010, **329**, 7-12.
87. M. Ghiaci, B. Aghabarari, A. M. Botelho do Rego, A. M. Ferraria and S. Habibollahi, *Appl. Catal. A*, 2011, **393**, 225-230.
88. X. Cai, H. Wang, Q. Zhang, J. Tong and Z. Lei, *J. Mol. Cat. A*, 2014, **383-384**, 217-224.
89. J. M. Fraile, J. I. Garcia, J. A. Mayoral and E. Vispe, *Appl. Catal. A*, 2003, **245**, 363-376.
90. S. N. Rao, K. N. Munshi and N. N. Rao, *J. Mol. Cat. A*, 1999, **145**, 203-210.
91. S. M. Mahajani, M. M. Sharma and T. Sridhar, *Chem. Eng. Sci.*, 1999, **54**, 3967-3976.
92. H. J. Neuburg, M. J. Phillips and W. F. Graydon, *J. Catal.*, 1975, **38**, 33-46.
93. K. Takehira, T. Hayakawa and T. Ishikawa, *J. Catal.*, 1980, **66**, 267-280.
94. P. Visuvamithiran, M. Palanichamy, K. Shanthi and V. Murugesan, *Appl. Catal. A*, 2013, **462-463**, 31-38.
95. M. M. T. Khan and R. S. Shukla, *J. Mol. Catal.*, 1990, **58**, 405-413.
96. S. Boudjema, E. Vispe, A. Choukchou-Braham, J. A. Mayoral, R. Bachir and J. M. Fraile, *RSC Adv.*, 2015, **5**, 6853-6863.
97. S. Sharma, S. Sinha and S. Chand, *Ind. Eng. Chem. Res.*, 2012, **51**, 8806-8814.
98. S. K. Pardeshi and R. Y. Pawar, *J. Mol. Cat. A*, 2011, **334**, 35-43.
99. M. Salavati-Niasari, E. Zamani and M. Bazarganipour, *Applied Clay Science*, 2007, **38**, 9-16.